Photopyroelectric (P^{2}E) Sensor for Trace Hydrogen Gas Detection

ANDREAS MANDELIS and CONSTANTINOS CHRISTOFIDES

Photoacoustic and Photothermal Sciences Laboratory, Department of Mechanical Engineering, and Center for Hydrogen and Electrochemical Studies (CHES), University of Toronto, Toronto, Ont., M5S 1A4 (Canada)

Abstract

A new type of solid-state sensor for the detection of minute concentrations of hydrogen gas has been developed. The sensor is made of thin, commercially-available polyvinylidene fluoride (PVDF) pyroelectric film, sputter-coated with Pd (or a Al–Ni double layer). We show that the device probably monitors the change in the pyroelectric coefficient of the film due to electrostatic interactions of adsorbed hydrogen ions with the VDF polymer matrix upon hydrogenation and selective absorption by the metallic coating. Presently, hydrogen concentrations as small as 0.075%, in a flowing $H_2 + N_2$ mixture, have been detected.

1. Introduction

In recent years, hydrogen gas has become a technologically important substance; it is used as a fuel in several industries, with the consequence that fast, *in situ* monitoring of trace amounts is of extreme importance. Therefore, a considerable research effort has been directed toward the development of hydrogen gas sensors. A number of gas sensors based on hydrogen-induced changes in the electrical conductivity of metal–oxide–semiconductor (MOS) structures have been reported [1–3]. Lundström *et al.* reported on Pd-gate MOS transistors and Pd-gate metal–insulator–semiconductor (MIS) sensors [4, 5]. Steele and MacIver showed that a Pd–CdS Schottky barrier diode exhibited a response to hydrogen [6]. The double metal-gate MISFET has also been used as a hydrogen sensor [7]. The insulate-gate field-effect transistor (IGFET) appears to have been successful as a hydrogen sensor as well [4, 8]. Hydrogen-sensitive MOSFETs with a catalytic gate metal, such as Pd [4], have also been reported. Furthermore, a variety of other hydrogen sensors have been developed: a surface acoustic wave (SAW) sensor [9], an optical fiber sensor [10] and a piezoelectric crystal detector [11]. A pyroelectric gas sensor, based on d.c. surface temperature changes due to heat of adsorption–desorption following

thermal ramping of the sensor, has also been reported [12]. This sensor requires a furnace-type environment for temperature ramping, and its sensitivity to trace gas analysis under dynamic, flow-through conditions has not been established. Severe noise problems due to surface temperature transients under flow conditions might be expected to limit the utility of this sensor. Zemel [13] has recently fabricated a $LiTaO_3$ pyroelectric detector, based on gas–surface interaction principles, which requires multi-level planar processing and is activated by resistive d.c. heating via a thin film (400 nm) NiCr heater. Besides its fabrication complexity, this d.c. pyroelectric sensor was proven to be extremely susceptible to temperature fluctuations due to environmental factors (e.g., valve opening and closing during gas cycles). An additional disadvantage of this (otherwise quite sensitive) sensor may be the long delay for gas detection (≈ 1 min) due to diffusive transport of thermal energy from the Pd electrode region to the reference (Au) electrode. These factors appear to have limited the development of purely pyroelectric devices as gas sensors to date.

This paper describes the development of a novel and simple thin-film photopyroelectric (P^{2}E) [14, 15] solid-state sensor for the detection of minute concentrations of hydrogen gas, with potentially superior sensitivity and speed of response. The present P^{2}E device is expected to solve many problems encountered with purely pyroelectric, and perhaps other, gas detectors, with the added element of fabrication simplicity.

2. Experimental

Poled PVDF thin films (β-phase) are known to exhibit strong pyroelectricity; i.e., a varying potential difference is generated (in the direction of poling) between the two metallized electrode surfaces that sandwich the pyroelectric film when a temperature change is induced within the pyroelectric layer [16]. The design of a hydrogen sensor fabricated from such a pyroelectric thin film has become feasible because of the ability of the pyroelectric to respond

to a.c. optical excitation, and the possibility of depositing a variety of thin metal electrode coatings on PVDF. For this work, our target was to coat PVDF with a metal which can adsorb and subsequently absorb hydrogen gas molecules preferentially in the presence of other ambient gases. Our hypothesis is that, upon establishing a steady-state temperature field within the pyroelectric by amplitude-modulated laser irradiation, any changes in the pyroelectric properties (and the pyroelectric coefficient in particular) of the PVDF, due to interactions with the hydrogen gas, will register as changes in the observed P^2E signal, thus yielding a hydrogen sensor.

It is well known that both palladium (Pd) and nickel (Ni) have high hydrogen solubilities, and that the effect is stronger in Pd [17]. Palladium, because of its selectivity to hydrogen absorption, has been employed as a filter for hydrogen purification [17], and has also been used to provide hydrogen selectivity for piezoelectric [11] and purely pyroelectric [13] hydrogen detectors.

A system has been constructed that allowed us to test the response of the Pd–PVDF pyroelectric sensor to flows of hydrogen/nitrogen mixtures, with H_2 concentrations ranging from pure nitrogen to pure hydrogen. The system consisted of four subsystems: gas control, temperature control, test cell and signal generation and analysis.

The heart of the system is the test cell: it contains two P^2E detectors (active Pd-coated and reference standard Pennwalt Al–Ni-coated electrode) [16]. The gas-handling system introduces a mixture of hydrogen and nitrogen gases into the test cell and allows the mixture to leave through the exhaust line after pumping. The temperature-control system ensures that the temperature of the incoming gas flow will be the same as that of the sensor itself. Care was taken in the design of the gas-flow chamber to ensure easy access of symmetric flow patterns over the active and reference detectors.

An overview of the experimental arrangement of the P^2E sensor is shown in Fig. 1(a). The instrumentation consisted of an RCA laser diode powered by an a.c. current supply. The output laser beam, 4 mW p-t-p multimode at ≈800 nm, was directed to a three-way fiber-optic coupler where it was split at approximately 16, 34 and 50%. Detailed schematics of the PVDF cells, active, A, and reference, B, as well as the feedback control are shown in Fig. 1(b). As is shown there, the 16% intensity fiber-optic channel was directed to a photodiode (PD) whose output was then sent to the 'monitor' input of the home-made laser current supply for preamplification and the feedback control of the laser current, as well as for synchronous lock-in detection. The feedback control consisted of using this reference signal to correct temporal intensity variations in the modulated laser beam. Only

a small fraction of the electrode areas is illuminated. The spots are approximately 0.8 mm in diameter, and could be controlled by moving the optical fibers closer to, or away from, the metallized surface. Note that the optical fibers guide the light very close to the Al–Ni–PVDF films (≈1–2 mm). In the same Figure information is given concerning the thicknesses of different coatings. According to Pennwalt Corporation [18], the Ni film on the PVDF is necessary because the Al does not adhere to VDF polymer. Before discussing the photopyroelectric response upon introduction of hydrogen, it is important to note that the gas contacts the Pd and Al–Ni surfaces only (see Fig. 1(a)–(c)) while the surfaces subjected to IR irradiation are isolated from the exposed gases. Small amounts of vacuum grease (visible in Fig. 1(c)) were placed at the entrance holes of the optical fibers into the PVDF housing, and ensured that the back illuminated area of the PVDF surface was sealed off from access by the H_2 gas in the chamber. The modulation frequency of the infrared beam was monitored with a frequency meter. It is important to note that the optical absorption of the metallized PVDF film in the infrared region of the spectrum is very high so that sensor operation was in the photopyroelectric saturation regime, independent of the optical properties of the coated PVDF [19]. The a.c. P^2E detector signals from a 28 μm thick PVDF film, on which a thickness of ≈285 Å Pd had been evaporated (henceforth designated 'unit A') and a similar PVDF film first covered with 200 Å standard Ni and then with 600 Å of Al [18] ('unit B'), were bandpass-filtered and preamplified by two low-noise pre-amplifiers. The two signals were then connected to a double-input oscilloscope for visual display, and to two lock-in analyzers, designated units 1 and 2 (see Fig. 1(a)). The lock-in amplifiers were referenced by the a.c. laser current supply. The output of lock-in 1 was connected to lock-in amplifier 2, which was equipped with a ratio option, allowing the absolute value of the normalized function output to be obtained [20]:

$$|\Delta S| = \frac{|V_A - V_B|}{|V_R|} \tag{1}$$

where V_A is the signal obtained from the Pd–PVDF electrode, V_B is the signal generated by the Al–Ni–PVDF electrode and V_R is the a.c. laser power reference output obtained from the photodiode PD. As shown in Fig. 1(a) and (b), in general two output infrared beams were directed to the Pd–PVDF and Al–Ni–PVDF films. The two pyroelectric transducers absorbed the thermal energy of the infrared beams and thus gave rise to two different electrical voltages, V_A and V_B.
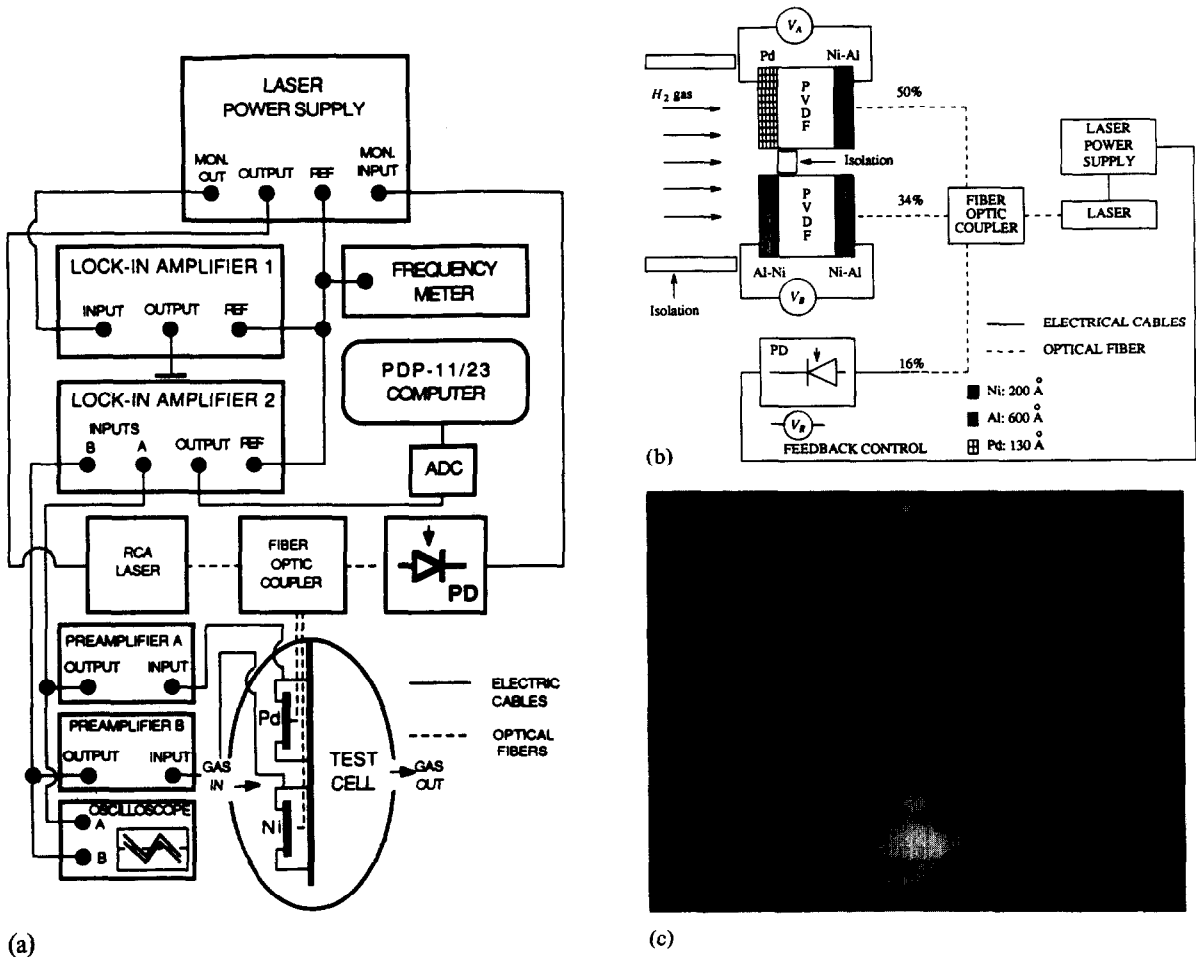
Fig. 1. (a) Schematic overview of the P²E sensor set-up. (b) Detail of the gas-flow chamber, including the active Pd-coated and reference Al–Ni-coated PVDF cells. (c) Photograph of the test cell chamber, showing the two photopyroelectric Inficon housings.

3. Analysis of the Photopyroelectric Response

Figure 2 presents the a.c.-induced photopyroelectric voltages, V_A and V_B, of the two PVDF films as displayed on a double-input Tektronix (model T912) oscilloscope. In our case, harmonic modulation of the beam intensity resulted in harmonic changes in ΔT (because of the harmonic change of the incident IR light fluence), which subsequently gave rise to synchronous a.c. voltages $V_A(f)$ and $V_B(f)$:

$$V_A(f) = \frac{\eta p_A W_A(f) E_{A_L}}{\epsilon C_A E_{Ael}} \qquad (2.1)$$

$$V_B(f) = \frac{\eta p_B W_B(f) E_{BL}}{\epsilon C_B E_{Bel}} \qquad (2.2)$$

where the subscripts A and B refer to the active (Pd) and the reference (Al–Ni) electrodes, respec-

tively; p_A and p_B are the pyroelectric coefficients; W_A and W_B are the incident optical fluxes; C_A and C_B are volume specific heats; η is the illuminated surface emissivity; ϵ is the PVDF dielectric constant; E_{AL} and E_{BL} are the illuminated areas; and E_{Ael} and E_{Bel} are the electrode areas ($E_{AL} < E_{Ael}$ and $E_{BL} < E_{Bel}$). The surface emissivity η is in fact a nonradiative efficiency factor, indicating the percentage conversion of optical energy to thermal energy. η in our case is very high due to the high absorptance of the Ni–Al metallized PVDF in the infrared region of the spectrum. From eqns. (1), (2.1) and (2.2), the output differential signal prior to the introduction of hydrogen gas in the test cell generated in the Pd–PVDF and the Al–Ni–PVDF electrodes may be written as

$$\Delta S(f) = \frac{1}{V_R} \frac{\eta}{\epsilon C} \left[\frac{p_A W_A(f) E_{AL}}{E_{Ael}} - \frac{p_B W_B(f) E_{BL}}{E_{Bel}} \right] \qquad (3)$$

Fig. 2. Photopyroelectric a.c. responses $V_A(f)$ and $V_B(f)$ of the two PVDF films as displayed on a double-input Tectronix oscilloscope. $V_A(f)$ and $V_B(f)$ have the same amplitudes (prior to the introduction of hydrogen gas) because of the choice of gain on the preamplifiers.

where $f = 20$ Hz and $C_A = C_B \equiv C$, due to the impermeability of the PVDF film bulk by hydrogen. The lock-in output channels were connected to a computer, through the ports of an A/D converter, for data storage and analysis of the ratioed output signal amplitude, ΔS. In eqn. (3) the absolute value signs have been replaced by brackets, because it was found that the active electrode signal V_A increased in the presence of H_2, while V_B remained unaltered.

Since the heat flows into the P^{2}E devices from the laser beams are not equal ($W_A \neq W_B$; see Fig. 1(b)), the two photopyroelectric voltages were different. Thus, the magnitude of ΔS was minimized in the beginning of each experiment by a judicious choice of gain on the preamplifiers, prior to introduction of the gas into the test cell ($V_B \approx V_A \rightarrow |V_B - V_A| \rightarrow \Delta S \approx 0$). As a result of the above considerations we can write that, initially

$$\frac{p_A[0]W_A E_{A_L}}{E_{A_{el}}} = \frac{p_B[0]W_B E_{B_L}}{E_{B_{el}}} \qquad (4.1)$$

where the bracketed quantities signify ambient H_2 concentration. The introduction of hydrogen into the test cell does not change the heat fluxes because $\Delta T(f)$ is solely determined by the infrared laser beams. Thus in the following discussion we shall assume that $W \equiv W_A = W_B$ because of the choice of gain on the preamplifiers. It is also clear that during the measurements, the distances of the optical fibers from the PVDF illuminated surface remain constant, and because of that we can also assume that the two areas are equal: $E_L \equiv E_{A_L} = E_{B_L}$. The relation (4.1), which is imposed because $\Delta S = 0$, may then be rewritten as

$$\frac{p_A[0]}{E_{A_{el}}} = \frac{p_B[0]}{E_{B_{el}}} \qquad (4.2)$$

Upon introduction of hydrogen into the test cell, a rise of the normalized differential voltage was caused by the H_2 (atomic or molecular) adsorption on, and absorption in, the palladium film. This normalized differential voltage is given by the relation

$$\delta S(f) = \frac{1}{V_R} \frac{\eta W(f)E_L}{\epsilon C} \left[\left(\frac{p_A[H]}{E_{A_{el}}} \right) - \left(\frac{p_B[H]}{E_{B_{el}}} \right) \right] \qquad (5)$$

In the absence of H_2 ($[H] = 0$), all the coefficients (pyroelectric coefficients, electrodes and illuminated areas and volume specific heats) of the two terms in eqn. (5) can be assumed identical. With the introduction of hydrogen into the chamber, if there is an increase of δS, eqns. (3)–(5) lead to a new relationship between the pyroelectric factors:

$$\frac{p_A[H]}{E_{A_{el}}} > \frac{p_B[H]}{E_{B_{el}}} \qquad (6)$$

From the above inequality one can conclude that the introduction of hydrogen into the test cell gives rise to a photopyroelectric response because of the change of the pyroelectric coefficient *and/or* the change of the effective palladium electrode area (change in the PVDF capacitance). In order to identify the more probable mechanism generating the hydrogen response, both possibilities will be examined separately.

Hypothesis 1: Response Due to the Change of the Pyroelectric Coefficients

We assume that $E_{el} \equiv E_{A_{el}} = E_{B_{el}}$. Before the introduction of the hydrogen ($[H] = 0$) the pyroelectric coefficients of the Pd- and Ni–Al-coated PVDF films may be assumed identical: $p_A[0] = p_B[0]$. Thus, for an interaction of H_2 gas with the Pd to cause an excess differential voltage δS, after hypothesis 1, eqn. (5) may be written as [14, 15]

$$\delta S = K_1(p_A[H] - p_B[H]) \qquad (7)$$

where K_1 ($\equiv \eta W E_L/\epsilon C E_{el} V_R$) is a system constant. However, $p_B[H] = p_B[0] \approx p_A[0]$, and this is due to the lack of response of the Al–Ni surface to H_2 gas. This shows that in the absence of hydrogen gas $\delta S = 0$. With the above considerations and writing $\Delta p_A \equiv p_A[H] - p_A[0]$, eqn. (7) may be modified:

$$\delta S(f) = K_1 \Delta p_A \qquad (8)$$

For small departures from the $p_A[0]$ value, the derivative of the pyroelectric coefficient p_A with respect to the density of absorbed atoms (or ions), N_H, gives the Δp_A variation [14, 15]:

$$\Delta p_A = \left(\frac{\partial p_A}{\partial N_H} \right)_{N_H = 0} N_H \qquad (9)$$

In eqn. (9) $(\partial p_A/\partial N_H)_{N_H=0}$ is a measurable material constant of the Pd-metallized PVDF. Using eqns. (8) and (9), in the saturation regime (i.e., $t \to \infty$: $\delta S \to \delta S_s$) we can write

$$\delta S_s = K_1 \left(\frac{\partial p_A}{\partial N_H} \right)_{N_H=0} N_{H_s} \tag{10}$$

where N_{H_s} is the saturated number of the adsorbed and absorbed hydrogen atoms/ions.

Hypothesis 2: Response Due to Change in the Effective Electrical Area

We assume that $p \equiv p_A = p_B$. Before the introduction of hydrogen, the areas of the two electrodes of the Pd- and Ni—Al-coated PVDF films may also be assumed identical: $E_{Ael}[0] = E_{Bel}[0]$. Thus, for interaction of H_2 gas with Pd to cause an excess differential voltage δS, according to hypothesis 2, eqn. (5) may be written as

$$\delta S = K_2 \left[\frac{1}{E_{Ael}[H]} - \frac{1}{E_{Bel}[H]} \right] \tag{11}$$

where K_2 ($\equiv \eta W p E_L/\epsilon C V_R$) is a system constant. However, $E_{Bel}[H] = E_{Bel}[0] \approx E_{Ael}[0]$, and this is due to the null response of the Al—Ni surface to H_2 gas. This shows that in the absence of hydrogen gas $\delta S = 0$. With the above considerations, writing $\Delta E_{Ael} = E_{Ael}[H] - E_{Ael}[0]$, and for small departures from the $E_{Ael}[0]$ value, eqn. (11) may be written

$$\delta S(f) \approx -K_2 \frac{\Delta E_{Ael}}{(E_{Ael}[0])^2} \tag{12}$$

Under these conditions, the derivative of the electrode area E_{Ael} with respect to N_H is the ΔE_{Ael} variation:

$$\Delta E_{Ael} = \left(\frac{\partial \Delta E_{Ael}}{\partial N_H} \right)_{N_H=0} N_H = \left(\frac{\partial E_{Ael}[H])}{\partial N_H} \right)_{N_H=0} N_H \tag{13}$$

Using eqns. (12) and (13), in the saturation regime

$$\delta S_s = -K_2 \frac{1}{(E_{Ael}[0])^2} \left(\frac{\partial E_{Ael}[H]}{\partial N_H} \right)_{N_H=0} N_{H_s} \tag{14}$$

4. Results and Discussion

Typical experimental results are shown in Fig. 3 for various hydrogen concentrations. Figure 3(a) and (b) shows typical P^2E responses as a function of time. These experiments have been performed under the same conditions (temperature: 20 °C, flow rate: 500 ml/min); note the variation of δS as a function of time for hydrogen concentrations ranging from
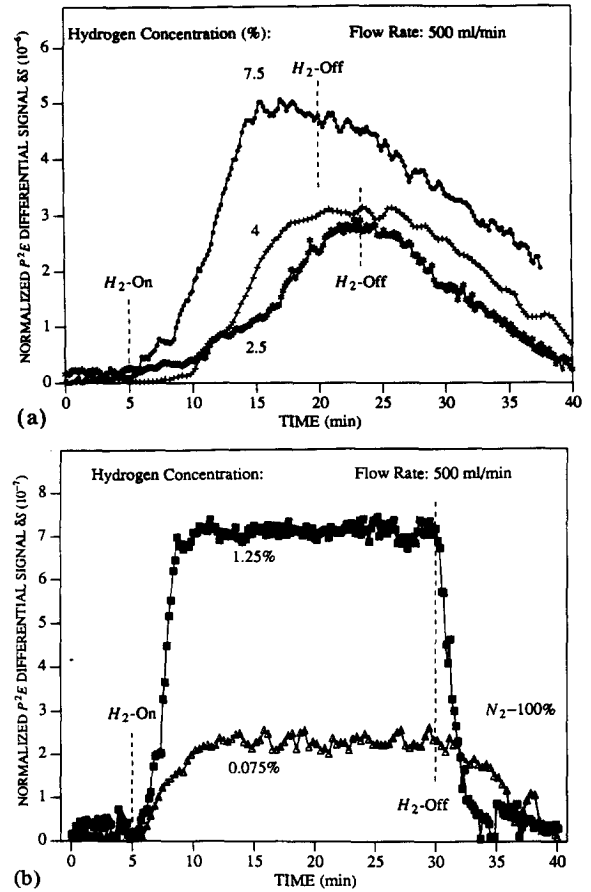

Fig. 3. P^2E responses as a function of time, for different concentrations of hydrogen in nitrogen ($T = 20$ °C): (a) 2.5 to 7.5% hydrogen; (b) 0.075 and 1.25% hydrogen. Pd thickness: 285 A (a); 130 A (b).

7.5 to 0.075% At the times indicated by the H_2-On markers, the sample gas was allowed to pass through the test cell. After saturation (horizontal part of the $\delta S(t)$ curves; t is the time) at the times indicated by the H_2-Off markers, pure nitrogen flowed continuously through the cell in order to remove the absorbed hydrogen. As a result, δS decreased to the baseline existing prior to the introduction of the sample gas. Figure 4 shows the variation of δS as a function of hydrogen concentration. It is important to realize that δS decreases significantly when the hydrogen concentration becomes lower than 10%. This concentration range corresponds to a hydrogen partial pressure between 7500 and 75 Pa. The sensitivity of the photopyroelectric sensor to such low hydrogen flow-through partial pressures makes it a promising detection device for trace hydrogen gas analysis under STP conditions, unlike the available MOSFET devices, which require operation in elevated temperature environments for enhancement in sensitivity and speed of response [4, 5, 21]. Most importantly, the lowest (0.075%) hydrogen concen-
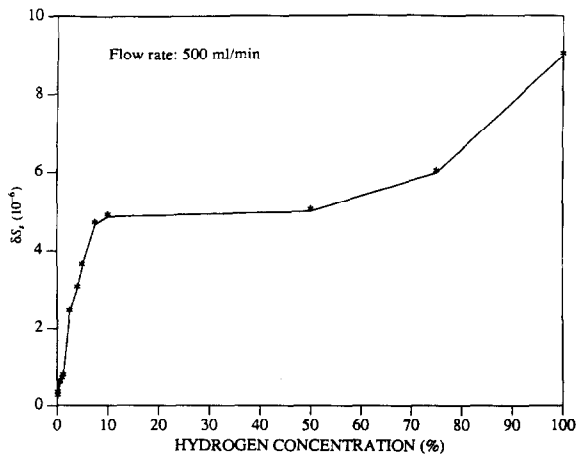
Fig. 4. Variation of output differential saturated signal amplitude δS_s as a function of hydrogen concentration ($T = 20$ °C).
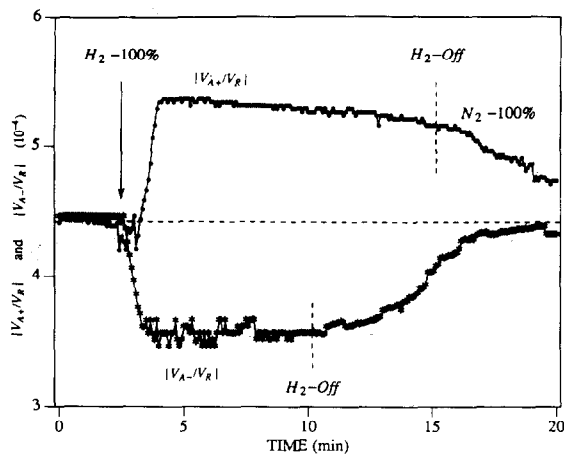

Fig. 5. (●) Variation of $|V_{A+}|/|V_R|$ as a function of time. (*) Variation of $|V_{A-}|/|V_R|$ as a function of time.

tration signal is not believed to be an absolute minimum. In fact, our most recent experiments have shown that detection of 40 ppm is possible at room temperature [22]. A future optimization of our set-up and detection electronics is expected to improve this level of sensitivity.

The likelihood of either hypothesis 1 or 2 being the major mechanism responsible for the P^2E sensor signal δS in the presence of H_2 was further examined. Toward this goal, two PVDF films were coated with 285 Å Pd on oppositely polarized surfaces. These films were used as detectors and Fig. 5 shows the time evolution of $|V_A|/|V_R|$ upon exposure to pure hydrogen. It can be seen that the positively polarized electrode gives an induced normalized voltage $|V_{A+}|/|V_R|$, which increases as a function of time (● points). The voltage from the negatively polarized electrode, $|V_{A-}|/|V_R|$, decreases as a function of time (* points) in a manner essentially

symmetric with respect to the equilibrium level (dashed line in Fig. 5). This experiment shows that the pyroelectric response is sensitive to the sign of the charges at the PVDF surface next to the Pd layer. The results are consistent with the presence of charged H^+ ions at the Pd—PVDF interface [21, 23, 24]. In the case of the positively polarized electrode, the additional positive charges (protons) will raise the electrostatic potential of the front surface with respect to the unexposed back surface. This would result in an increased photopyroelectric voltage, as observed. On the contrary, absorbed protons are expected to neutralize (cancel) the field due to the negative charges at the surface of the negatively polarized electrode, thus lowering the electrostatic potential of the front surface. This would result in the observed decreased P^2E voltage. The above picture is corroborated by mechanistic evidence available from other solid-state Pd-coated hydrogen sensors, which operate as back-interface detection devices similar to the new Pd—PVDF sensor. Specifically, with the Pd—MOSFET, upon dissociation at the Pd surface, hydrogen enters the Pd bulk as ions (protons, H^+) and quickly migrates to the interface where it shifts the gate bias [21, 23] due to the device interactions with the H^+ charge. A certain spillover in the insulating SiO_2 layer of the MOSFET has also been detected [21, 23]. It thus appears that our hypothesis 1 offers a valid operational description of the Pd—P^2E sensor.

Figure 6 shows the P^2E signal δS evolution in the case where H_2 access to the back (illuminated) surface of the sensor PVDF film was allowed. The film was coated with 285 Å Pd on both sides and pure hydrogen gas was introduced into the test cell at $t = 1$ min. An initial differential signal appeared, which after reaching a maximum returned to the baseline while hydrogen was still flowing. It is evident that the transient is due to the delayed H_2 arrival
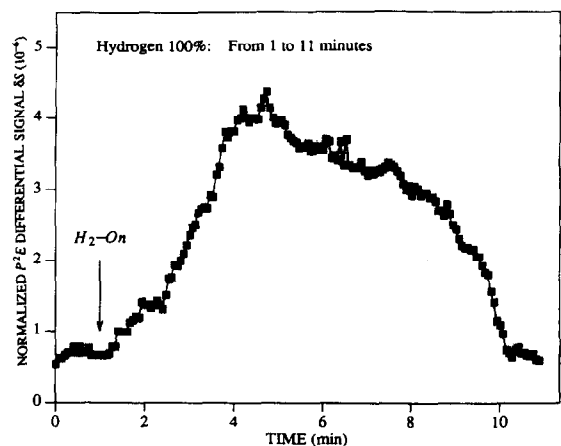

Fig. 6. Exposure of Pd—PVDF—Pd film to hydrogen on both sides. Variation of δS as a function of time.
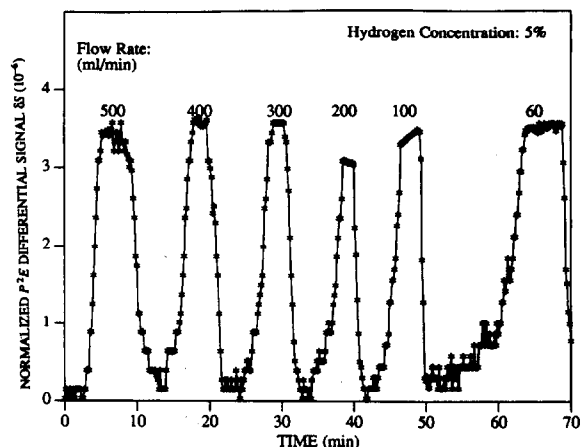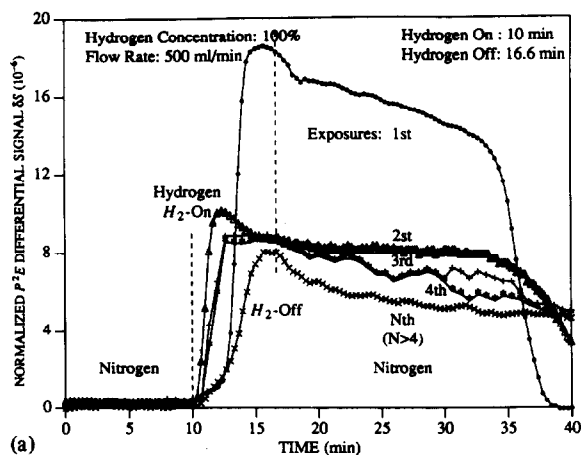
Fig. 7. Variation of output differential signal amplitude δS as a function of time for various hydrogen flow rates (60 to 500 ml/min; $T = 20\ ^\circ$C).

at the back surface of the Pd–PVDF film. Once in contact with both metal–polymer interfaces, the extraneous electrostatic charge densities at the front surface, which generated the initial differential voltage, were entirely compensated by similar charges in the symmetric geometry of the back surface, thus returning the observed voltage to the pre-exposure level. It should be noted that the steady-state saturation δS levels of the sensor with one surface exposed to H_2, and the return of the δS level to the baseline of the sensor with two exposed surface, are indicative: (i) of the impermeability of PVDF bulk to hydrogen and (ii) of the invariance of the photothermal signal with the incorporation of hydrogen in the Pd matrix of the illuminated surface.

Figure 7 shows the variation of δS as a function of time for different H_2 flow rates (500 to 60 ml/min), $T = 20\ ^\circ$C, H_2 concentration = 5% in nitrogen). Note that the flow rate does not influence the overall δS behavior very much, and saturation occurs essentially at the same level. On the other hand, the flow rate does influence the response time of the sensor, which increases monotonically (3 min to 10 min) with decreasing flow rate between 500 ml/min and 60 ml/min.

The experimental results show that our Pd–PVDF P^2E sensor is completely reversible and durable. Initially, one face of the Pd–PVDF film (285 Å) was exposed several times to 100% H_2 (10^5 Pa). The experimental curves in Fig. 8(a) show an irreversible sensitivity loss with each successive introduction of hydrogen. A similar phenomenon has been observed by Lalauze *et al.* [25] using pure Pd substrates. According to these authors, sample treatment (exposure and heat treatment) has a large influence on hydrogen adsorption. Our Pd–PVDF P^2E signal saturated at a reproducible value after four of five exposures (Fig. 8(a)) without any additional treat-
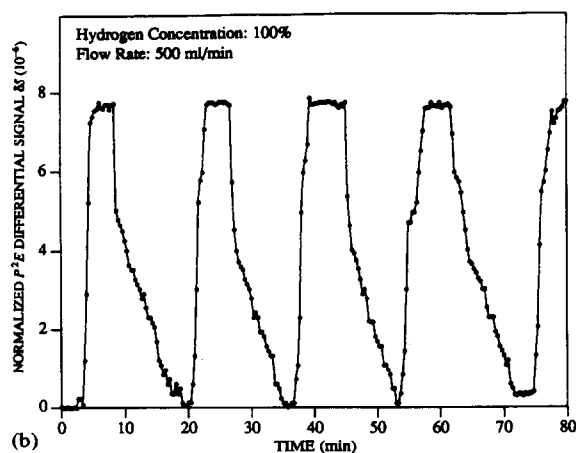
Fig. 8. Variation of output differential signal amplitude δS as a function of time, after several exposures to pure hydrogen ($T = 20\ ^\circ$C). (a) With an as-received Pd–PVDF film; (b) with a previously exposed Pd–PVDF film.

ment, unlike the work by Lalauze *et al.*, who reported stabilization only after a relatively sophisticated treatment program had been followed. The stability of our sensor has been repeatedly confirmed with three different Pd–PVDF films. Figure 8(b) shows the excellent reproducibility of the signal after many exposures to pure hydrogen following the first five 'break-in' exposures. The signal level has been found to be very reversible and reproducible with several Pd–PVDF films. In terms of durability, the basic signal quality shown in Fig. 8(b) lasted for several hundred exposures, as well as under various hydrogen concentrations. Thus, reproducibility and durability of the photopyroelectric sensor have been successfully demonstrated in this work.

Conclusion

In this paper, the first photopyroelectric gas detector has been presented. Our first experimental

results suggest that a new Pd–PVDF P^2E sensor can be implemented as a trace hydrogen detector, under ambient conditions or in remote locations. A study of the sensitivity limits, speed of response, reproducibility, durability and simplicity has been performed. An analysis of the variation of the photopyroelectric normalized differential signal after exposure to hydrogen has been carried out by examining separately the probable signal-generating factors of the P^2E device, such as the pyroelectric coefficient and the electrode area (capacitance of the film).

The main results of our study can be summarized as follows:

(1) The room-temperature operation capability of the new P^2E sensor may be indicative of comparable (or even superior) performance to those of several other purely pyroelectric gas sensors, and, perhaps, other solid-state hydrogen detectors mentioned in the introduction to this work. For instance, the room-temperature operation capability of the new P^2E sensor may be indicative of superior durability over the Pd–MOSFET, which requires elevated operating temperatures [4, 5, 21, 23] for high sensitivity and speed of response. Further results in comparison with a piezoelectric crystal detector will be presented elsewhere [26].

(2) The present results are consistent with the hypothesis that the photopyroelectric device monitors the change in the photopyroelectric coefficient of the film due to electric dipole coupling between hydrogen ions and the VDF polymer matrix upon hydrogenation and selective absorption by the metallic coating.

(3) The detector has been found to be reversible and durable. The Pd–PVDF film has shown a reversible response for several hundred adsorption–absorption–desorption cycles.

Extensions of the present measurements to the detection of other gases may lead to an increase of the P^2E detector utilization: other environmentally important gases may be detectable, such as hydrocarbons, SO_2, HCl, NH_3, H_2S, and even radioactive gases such as tritium with appropriate metallic electrode coatings.

The hydrogen P^2E sensor has the potential to become an excellent tool for surface science studies under UHV conditions, for example, for heat of adsorption measurements of the Pd–H_2 system, especially at low temperatures where other hydrogen detectors do not exhibit good operating characteristics.

Acknowledgements

References

1 T. Seiyama and S. Kagawa, Detector for gaseous components with semiconductive thin films, *Anal. Chem.*, *38* (1966) 1069–1073.
2 P. J. Shaver, Activated tungsten oxide gas detector, *Appl. Phys. Lett.*, *11* (1967) 255–257.
3 H. Obayashi, Y. Sakurai and T. Gejo, Perovskite-type oxide as ethanol sensors, *J. Solid State Chem.*, *17* (1976) 299.
4 K. I. Lundström, M. S. Shivaraman and C. M. Svensson, A hydrogen-sensitve Pd-gate MOS transistor, *J. Appl. Phys.*, *46* (1975) 3876–3881.
5 K. I. Lundström, M. S. Shivaraman and C. M. Svensson, Chemical reactions on palladium surfaces studied with Pd-MOS structures, *Surf. Sci.*, *64* (1977) 497.
6 M. C. Steele and B. A. MacIver, Palladium/cadmium-sulfide Schottky diode for hydrogen detection, *Appl. Phys. Lett.*, *28* (1976) 687–688.
7 T. Yamamoto and M. Morimoto, Thin-MIS-structure Si negative-resistance diode, *Appl. Phys. Lett.*, *20* (1976) 269–270.
8 T. L. Poteat and B. Lalevic, Transition metal-gate MOS gaseous detectors, *IEEE Trans. Electron Devices*, ED-29 (1982) 123–129.
9 A. D'Amico, A. Palma and E. Verona, Palladium-surface acoustic waves, *Appl. Phys. Lett.*, *41* (1982) 300–301.
10 M. A. Butler, Optical fiber hydrogen sensor, *Appl. Phys. Lett.*, *45* (1984) 1007–1009.
11 S. Abe and T. Hosoya, Detection of hydrogen in ambient air using a coated piezoelectric crystal, *Proc. 5th World Hydrogen Energy Conf., Toronto, Ont., Canada, July 15–20, 1984*, Vol. 4, pp. 1893–1900.
12 J. N. Zemel, B. Keramati and C. W. Spivak, Non-FET chemical sensors, *Sensors and Actuators, 1* (1981) 427–473.
13 J. N. Zemel, in J. Janata and R. J. Huber (eds.), *Solid State Chemical Sensors*, Academic Press, New York, 1985, Ch. 4, pp. 188–207.
14 A. Mandelis and C. Christofides, Photopyroelectric solid state sensor for hydrogen gas trace detection, *Conf. Digest 6th Int. Topical Meet. Photoacoustic and Photothermal Phenomena, Baltimore, MD, U.S.A., July 31–Aug. 3, 1989*, pp. 352–353.
15 C. Christofides and A. Mandelis, Development of a new photopyroelectric solid state sensor for hydrogen gas detection, *IEEE 1989 Ultrasonics Symp., Montreal, Quebec, Canada, Oct. 3–6, 1989*, in press.
16 *KYNAR Piezo Film Technical Manual*, Pennwalt Corp., King of Prussia, PA, 1983.
17 F. A. Lewis, in *The Palladium/Hydrogen System*, Academic Press, New York, 1967, pp. 1–12.
18 R. Ferren (Engineering Manager), Pennwalt Corp., King of Prussia, PA, personal communication, June 1989.
19 A. Mandelis and M. Zver, Theory of the photopyroelectric effect in solids, *J. Appl. Phys.*, *57* (1985) 4421–4430.
20 *Operating and Service Manual*, EG&G Princeton Applied Research, model 5204 (lock-in Analyzer); *Ratio Option*, pp. 23–24.
21 K. I. Lundström, M. Armgarth and L.-G. Petersson, Physics with catalytic metal chemical sensors, *CRC Critical Rev. Solid State Mater. Sci.*, *15* (1989) 201–278.
22 C. Christofides and A. Mandelis, Operating characteristic and comparison of photopyroelectric sensors for trace hydrogen gas detection. Part 1: Development of a new photopyroelectric sensor, *J. Appl. Phys.*, *66* (1989) 3975–3985.
23 K. I. Lundström, Hydrogen sensitive MOS structures.

Part 1: Principles and applications, *Sensors and Actuators, 1* (1981) 403–426.

24 M. Armgarth, C. Nylander, C. Svensson and I. Lundström, Hydrogen-induced oxide surface charging in palladium-gate metal–oxide–semiconductor devices, *J. Appl. Phys., 56* (1984) 2956–2963.

25 R. Lalauze, P. Gillard and C. Pijolat, Hydrogen permeation through a thin film of palladium: Influence of surface impurities, *Sensors and Actuators, 14* (1988) 243–250.

26 C. Christofides and A. Mandelis, Operating characteristic and comparison of photopyroelectric sensors for trace hydrogen gas detection. Part 2: Piezoelectric quartz crystal microbalance sensor, *J. Appl. Phys., 66* (1989) 3986–3992.

Biographies

Andreas Mandelis was born on June 22, 1952, in Kerkyra (Corfu), Greece. He received the B.Sc. degree in physics in 1974 from Yale University. He received the M.A. degree in applied physics in 1976, the M.S.E. degree in mechanical and aerospace engineering in 1977 and the Ph.D. in applied physics in 1979 from Princeton University, Princeton, NJ.

He was a member of the scientific staff (silicon R & D) at Bell Northern Research, Ottawa, Ont. Canada, from 1979 to 1981. He then was an assistant professor in the Department of Mechanical Engineering at the University of Toronto, Toronto, Ont. Canada, from 1982 to 1986. He is currently an associate professor and director of the Photoacoustic and Photothermal Sciences Laboratory.

Dr Mandelis is a member of the American Physical Society, Sigma Xi, Canadian Association of Physicists, Spectroscopy Society of Canada, the New York Academy of Sciences, IEEE and the ASME.

Constantinos Christofides was born on January 13, 1959, in Nicosia, Cyprus. He received the Licence degree (B.Sc.) in physics in 1982 and the Maitrise degree (M.Sc.) in 1983 from Grenoble University (France). In 1984 he received the D.E.A. degree in energy-physics from the National Polytechnic of Grenoble (I.N.P.G.). A year later, he received the D.E.A. degree in economic energy from the University of Social Science in Grenoble. In 1986 he received the Ph.D. in applied physics from the National Polytechnic of Grenoble.

He is currently research associate at the University of Toronto. His major research interests are in the development of a new photopyroelectric hydrogen detector, infrared spectroscopy, photothermal laser deflection spectroscopy (PTR) and electrical measurements for the characterization of semiconductors.

Dr Christofides is a member of the American Physical Society, Canadian Association of Physicists and the International Solar Energy Society.